International Journal of Production Economics 204 (2018) 18–29

Contents lists available at ScienceDirect

International Journal of Production Economics

journal homepage: www.elsevier.com/locate/ijpe

Liquefied natural gas inventory routing problem under uncertain weather conditions

Jaeyoung Cho[a,*], Gino J. Lim[b], Seon Jin Kim[b], Taofeek Biobaku[c]

[a] Department of Industrial Engineering, Lamar University, Beaumont, TX 77710, USA
[b] Department of Industrial Engineering, University of Houston, Houston, TX 77204, USA
[c] Praxair, Tonawanda, NY 14150, USA

ARTICLE INFO

Keywords:
Liquefied natural gas
Maritime transportation
Inventory routing problem
Stochastic programming
Disruption management

ABSTRACT

We study the liquefied natural gas (LNG) production-inventory control and vessel routing problem under disruptive weather conditions. If extreme weather is expected to strike an LNG plant, all planned LNG loading operations should be rescheduled to prevent expected safety accidents. We propose two mathematical optimization models to cope with the potential disruptions. The first model is formulated as a two-stage stochastic mixed integer program to maximize the overall expected revenue while minimizing the cost caused by the uncertain impact of weather disruptions. The second model is a decision maker's preference model that reflects a decision maker's evaluation of risk. This model enables a decision maker to have a 'what-if' analysis by varying the level of preference for risks. The two proposed mathematical models can be reduced to a vehicle routing problem which is an NP-hard combinatorial optimization problem. Therefore, two computational techniques have developed to improve the optimization performance. First, a probing-based preprocessing technique is developed to reduce the solution space by eliminating obvious infeasible or non-optimal solutions. Second, an optional logical inequality is developed to generate an upper bound for the optimal solution only if an LNG carrier visits one or two customers in a single tour. Computational results indicate our proposed models and computational techniques are well suited to solve the problem within a reasonable time.

1. Introduction

In the last decade, there has been a remarkable upward trend in the LNG industry (Finley, 2014). To meet the growing international demand, North America has significantly increased its production of shale gas (U.S. Department of Energy, 2005; U.S. Energy Information Administration, 2014). Since February 2016, the U.S. began exporting LNG for the first time. This meant that the US, the world's largest natural gas consumer and importer, was now turning into a natural gas exporter.

Generally, natural gas is transported to customers either through pipelines or by a fleet of LNG carriers. The trade of natural gas through the pipeline is convenient and economical up to 2500 km. However, as shipping distances increase above this maximum, maritime transportation of natural gas in liquid form become more economical (Hartley et al., 2013; Hartley, 2014). LNG demand has been mostly identified from well-determined long-term contracts which have 20–30 year durations which guarantee stable supply and demand relations. Therefore, an annual delivery program was considered to fulfill a set of long-term contracts (Rakke et al., 2011). In recent years, however, there has been an increasing trend for spot-demand and short-term contracts. Traders are willing to trade at short notice when there is an increasing risk of holding surplus LNG unsold under long-term contracts. This trend change is similar to the global market for crude oil seen in the 1970s (Von Hirschhausen and Neumann, 2008).

The LNG value chain is composed of three phases as shown in Fig. 1 (Tusiani and Shearer, 2007). First, once natural gas is produced, it is stored in a storage tank in a liquid form at a temperature of −160 °C. The volume of natural gas in the liquefied state is 1/600 of the volume of the natural gas in its gaseous state. Second, LNG is transported from a production site to a consumer site by an LNG carrier. Usually, a certain amount of LNG is vaporized during the marine transportation. This boil-off gas (BOG) is considered a loss that cannot be delivered to consumers. Third, when an LNG carrier arrives at a consumer site, LNG is transformed back to its original gaseous state for ground transportation and distribution (Thomas and Dawe, 2003). The cost structure of each phase related to the LNG value chain is as follows: exploration & production ($0.60–1.2 per one million British thermal units, or MMBtu),

* Corresponding author.
E-mail addresses: jcho@lamar.edu (J. Cho), ginolim@uh.edu (G.J. Lim), sonjin64@gmail.com (S.J. Kim), tobiobaku@uh.edu (T. Biobaku).

https://doi.org/10.1016/j.ijpe.2018.07.014
Received 18 January 2018; Received in revised form 10 July 2018; Accepted 15 July 2018
Available online 30 July 2018

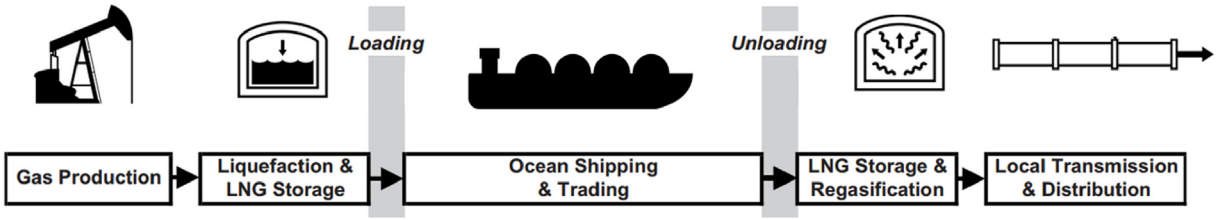

Fig. 1. LNG value chain.

liquefaction ($0.90–1.30/MMBtu), shipping ($0.50–1.80/MMBtu), storage & regasification ($0.40–0.60/MMBtu). The LNG value chain can be directly or indirectly affected by the following performance indicators: daily production rate, daily minimum and maximum regasification rate, initial inventory, storage capacity, volume loaded/discharged by ship, travel time between two terminals, demands, number of berths at a terminal, penalty for unmet demand at a terminal, penalty for lost production/stockout at a terminal, daily boil-off rate, LNG carrier operating cost, and port/terminal fees (Michot Foss, 2007; Goel et al., 2012, 2015; Andersson et al., 2010). This study covers the first and second phases of the LNG value chain to optimize LNG production, storage and LNG shipping scheduling at the same time, and this problem is classified as an LNG inventory routing problem (IRP).

The IRP is an integration of the production-inventory problem and the vehicle routing problem (VRP). The very first IRP was formulated as a mixed integer program to manage industrial gases at customer locations (Bell et al., 1983). Major applications of IRP are usually in the oil and gas industries because of the maritime shipping environment. From the perspective of ship routing and scheduling, the problems can be categorized into four basic models: 1) network design, 2) fleet deployment, 3) tramp cargo routing and scheduling problem and 4) maritime IRP for a single product (Christiansen et al., 2013). The fourth model is the focal point of this research.

Ship routing and production-inventory planning in the LNG business is a representative maritime IRP. While optimizing inventory and production levels within a given time horizon, a fleet of LNG carriers must be properly assigned to a path between a liquefaction terminal and a single or multiple regasification terminals.

There has been an increasing trend of research on LNG IRP since 2009. One of the earliest approaches reported in the literature was a mixed integer programming (MIP) model considering LNG cargo ships shuttling from a liquefaction plant to a regasification plant. These were formulated in an arc-flow and a path-flow model considering inventories at liquefaction and regasification terminals (Grønhaug and Christiansen, 2009). Subsequent models have evolved to become more realistic and progressive, with additional considerations such as sailing conditions, contract types and classes of LNG carriers (Andersson et al., 2010; Fodstad et al., 2010). Yet, a drawback of their studies is that they are limited to serving one customer in a tour. Traditional LNG demand is mostly identified from well-determined long-term contracts, and so an annual delivery program (ADP) was considered with a limited number of berths, and a heterogeneous fleet of LNG ships to fulfill a set of long-term contracts (Rakke et al., 2011). However, this model is not suitable when considering spot-demand and short-term contracts.

Because the LNG IRP is a complex optimization problem under various conditions, existing studies on optimization were focused on developing exact and approximate algorithms to reduce computational time to find a solution. For example, the Lagrangian relaxation technique was used to solve an LNG IRP with 800,000 variables and 200,000 constraints with the optimality gap of 0.5% (Bell et al., 1983). Other useful exact algorithms include branch-and-price (Grønhaug et al., 2010), branch-price-and-cut (Engineer et al., 2012; Coelho and Laporte, 2013), decomposition (Papageorgiou et al., 2014), and approximate dynamic programming (Papageorgiou et al.). A number of efficient heuristic approaches have also been proposed for the problem such as iterative heuristic search algorithm (Goel et al., 2015), multi-start construction and improvement heuristic (Stålhane et al., 2012), a route construction heuristic (Vidović et al., 2014), and a rolling horizon heuristic (Rakke et al., 2011).

In practice, the LNG IRP is significantly affected by various uncertainties. One of the most challenging problems is accurately forecasting uncertain demand. A simple way to approximate demand is to average recent customers' inventory levels as a constant (Bell et al., 1983), or to consider the demand as a random element (Federgruen and Zipkin, 1984). Even if the demands are known, disruptions from the supplier side can still make a value chain unstable (Baghalian et al., 2013). Another issue is volatile market prices which influences the production-inventory decisions (Arvesen et al., 2013). In maritime transportation, sailing time is inherently uncertain because of changing weather conditions (Halvorsen-Weare et al., 2013; Zhang et al., 2015).

Due to a constantly changing external environment during marine transport, LNG is randomly vaporized (Cho et al., 2014a). Since the vaporizing gas increases the pressure inside the storage tank, it is usually discharged to the outside for safety purposes. As an LNG carrier loses a fraction of gas during the voyage, the LNG supplier should consider both the amount of LNG to be delivered to the customer and the expected loss of random BOG generation at the time of determining the amount of LNG to be loaded on an LNG carrier. In an early stage of research, the focus was on discovering the characteristics of BOG in a partially filled tank and developing mathematical foundations (Chatterjee and Geist). In addition, the occurrence and the effect of BOG on the LNG value chain have been examined dividing the time phases into three categories: loading, unloading and marine transportation (Dobrota et al., 2013). Numerous environmental factors influence the degree of BOG generation. However, since the exact prediction of the BOG is too complex, it is often considered as a constant (Grønhaug et al., 2010; Zhang et al., 2015; Cho et al., 2014b).

Uncertain weather conditions disrupt LNG loading operations frequently. When severe weather is imminent, all port operation schedules related to LNG shipping, loading, production, and storage should be delayed or accelerated altogether to avoid safety accidents (Halvorsen-Weare et al., 2013; Zhang et al., 2015).

The literature review reveals that there is a clear need to study the impact of uncertain weather conditions on LNG IRP more carefully. Especially, no mathematical optimization models have been developed to minimize the impact of uncertain weather disruptions on the LNG value chain. To address this gap in the literature, we propose two mathematical optimization models to minimize the impact of extreme weather on the LNG value chain. The LNG IRP models generally include a very large number of variables, and require a significant computational time in order to solve the medium- and large-size instances to the global optimality. Therefore, we propose an approach that is computationally efficient to solve the optimization models in a reasonable time. Contributions of this paper can be highlighted as follows:

- A two-stage stochastic LNG IRP (TSS) model has been developed considering the uncertain occurrence time of bad weather which disrupts LNG production, storage, and shipping schedules. In a previous study, boil-off-rate (BOR) was considered as a random element (Cho et al., 2014b). However, BOR is set as a constant to

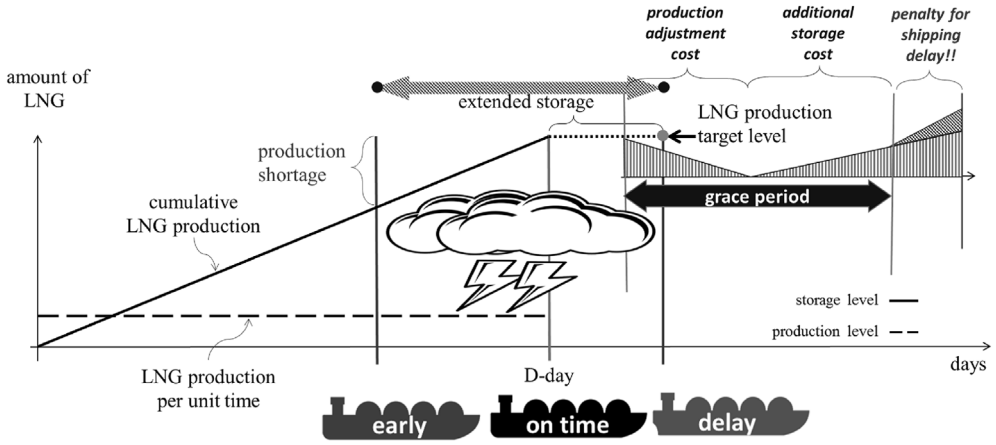

Fig. 2. A random extreme weather impacts to LNG production & storage plan and vessel departure time.

focus primarily on the impact of extreme weather as a significant disruption element in LNG shipping scheduling. This is a reasonable assumption because the impact of uncertain extreme weather has a substantially higher impact than that of uncertain BOR.

- A decision maker's preference (DMP) model has been proposed to reflect a decision maker's subjective perceptions on random weather events. If historical data on extreme weather is unreliable or insufficient, it is difficult to estimate the support of a probability distribution to generate reasonable weather scenarios. The DMP model reflects a decision maker's subjective ideas on weather scenario generation by using a triangular distribution.
- A probing-based preprocessing technique (PPT) has been developed to improve convergence speed to the optimal solution of the LNG IRP model. PPT utilizes the results by analyzing the relationship between the sailing time of LNG carriers operating at any two terminals and the demand time window at the destination where LNG reception is desired. Since TSS is a highly complex two-stage stochastic MIP model, this approach reduces the size of solution space and enables the model to be solved faster.
- An optional logical inequality is developed to generate an upper bound on the optimal solution only if an LNG carrier visits one or two customers in a single tour. This logical inequality not only eliminates the need of tour sequencing decisions for path planning but also enhances the computational performance.

The remaining sections of this paper are organized as follows. Section 2 describes the LNG inventory routing problem. Section 3 presents the proposed mathematical formulations of TSS and DMP followed by PPT and rPPT. Section 4 discusses computational results. We conclude the paper with discussions of opportunities for extensions of our work in Section 5.

2. Problem statement

The general goal of the LNG IRP is to provide an optimal production inventory schedule and transportation plans that satisfy all demands from customers in an LNG supply chain considering the terms and conditions of their contracts. LNG contracts typically include the duration of a contract, the frequency of delivery, the total amount of demand, expected shipping dates and locations, the grace period and any associated penalties for delays. In order to maximize the expected revenue, an LNG supplier has to consider various aspects such as maximum capacities for production and storage, the total number of LNG carriers per type, and the shipping schedule.

For the scheduling of multiple LNG carriers, while satisfying various demands, such as spot demand and long-term and short-term contracts, we consider two types of LNG carriers, following the specification of cargo tanks with or without restrictions on cargo loading. The first vessel type has a barred filling limit of LNG cargo which is categorized as type I. It has a permissible range that is either more than 70% or less than 10% of the tank. This exact filling limit is due to the sloshing effect which increases potential risks such as gas leaks and other related safety accidents (Cho et al., 2014b). The second vessel type (type II) is not limited to this filling limit for its cargo. It is flexible to any level of partial loading which allows for numerous cargo discharges at multiple regasification plants in a voyage path (Kuo et al., 2009; Rudman and Cleary, 2009).

Unlike other products, an LNG cargo evaporates gas during marine transport. The amount of evaporated gas is proportional to the amount of LNG cargo on board and the total cargo transit time. Therefore, the loading amount of LNG from a departing liquefaction plant must aggregate the total amount of LNG to be delivered and the estimated BOG loss during a voyage.

Extreme weather, such as a dust storm with strong winds in the Persian Gulf can make the LNG loading operations unstable. In general, any severe weather event can be predicted three days in advance and the LNG loading operations take about 12–18 h (UNEP Global Environmental Alert Service; Canaport; Qatar Petroleum).

There are two kinds of relationships between extreme weather and an LNG loading schedule as illustrated in Fig. 2. First, if severe weather is expected to impact the LNG loading start time, then a planned loading schedule must be altered. Due to the loading delay, an LNG cargo in the ground facilities must remain in storage for an extended period of time until the facility is open again after the weather disruption, which incurs an additional storage cost. Second, if a storm is expected to begin before the end of a planned loading operation, then the loading schedule must be adjusted so that the loading can be completed before the beginning of the storm. In this case, the LNG stock level will be lower than the planned amount because the production inventory schedule was originally aimed to meet the LNG stock level at a later date. Therefore, additional production efforts must be made at a higher cost to meet the demand.

The LNG supply network in this problem includes three routes: an initial delivery route, intermediate route(s) and a return route as shown in Fig. 3. An initial delivery route connects a liquefaction plant to a regasification plant while the return route follows the reverse order. An intermediate route links two regasification plants. Therefore, the intermediate route(s) can be included only if there are at least two regasification plants to visit in a path. When a vessel starts a voyage through an initial delivery route, the departure time from a liquefaction plant can vary depending on the expected arrival time of an extreme weather condition and its estimated duration.

There are seven categories of decision variables involved in the problem: 1) the amount of LNG to be delivered to each customer per

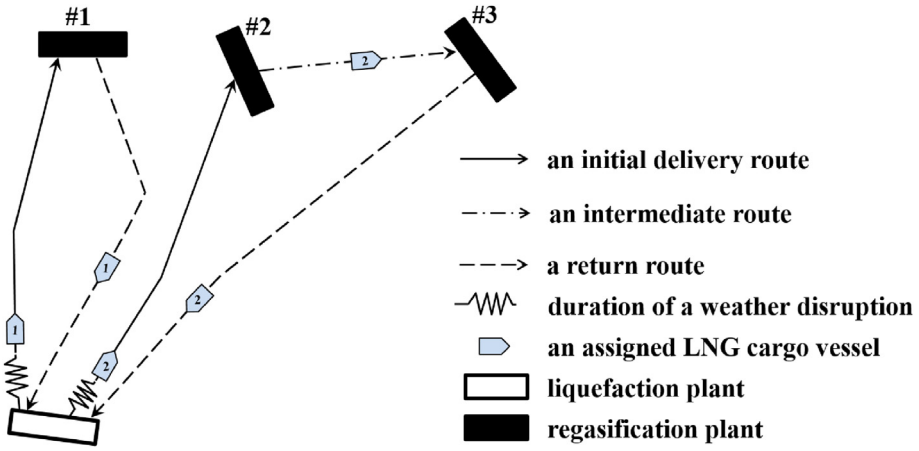

Fig. 3. Three types of transportation routes connecting plants.

carrier, 2) the vessel assignment to a travel path, 3) the daily inventory and production schedule, 4) departure and arrival times of an incoming and outgoing vessel at each regasification plant, 5) the number of delay days, 6) the amount of additional LNG production anticipating an LNG inventory shortage and 7) the amount of excessive LNG or shortage after the realization of a random weather disruption.

3. TSS model and solution methods

We formulated our TSS model as a two-stage stochastic program as we consider uncertain weather conditions. In general, solving a stochastic program is computationally challenging due to the existence of random parameters that follow a continuous probability distribution. Alternatively, the stochastic program can be solved by using a discrete set of scenarios to represent the random events. If the scenario set is small, then the model can be solved with deterministic problem solution techniques without the loss of optimality (Higle et al., 1990). As the set of weather disruption scenarios Ω is assumed discrete and finite in a TSS model, we present a deterministic equivalent of a two-stage stochastic LNG IRP. Sets, data, random elements, and decision variables used for the mathematical formulation of a TSS model are defined as follows:

Let $G(V, A)$ be a directed network, where V is the set of LNG plants and A is the set of vessel routes. A supplier at a liquefaction plant $i_0 \in V_1$ delivers demanded LNG cargo D_j to a customer at a regasification plant $j \in V_2$ by LNG carrier $k \in K$ through the traverse arc $(i, j) \in A$. Any path is composed of the initial delivery route A_1, intermediate route A_2 and return route A_3. An LNG supplier delivers the ordered demands $|r_s|$ to its customers within the periods specified in the LNG supply contract. The most appropriate LNG carrier $k \in K$ is assigned for LNG shipping. Recall that there are two types of vessels: type I vessel $k_1 \in K_1$ and type II vessel $k_2 \in K_2$ where $K = \{K_1 \cup K_2\}$ and $K_1 \cap K_2 = \emptyset$. A type I vessel has to strictly follow the barred cargo fill range $[\underline{\alpha}, \overline{\alpha}]$, but a type II vessel has no restrictions on its cargo scale. When an LNG carrier $k \in K$ makes a tour visiting multiple regasification plants, the sequence of visits is determined by introducing an extra variable u_i for each plant $i \in V_2$. Daily production level x_t^{prd} and inventory level x_t^{str} are determined considering maximum production capacity $\overline{\psi}$ and minimum production level $\underline{\psi}$, and maximum storage capacity $\overline{\rho}$ and minimum safety stock level $\underline{\rho}$ respectively. LNG volume D_i ordered by a customer $i \in V_2$ is delivered between the expected target delivery date and additional grace days E_i^{tot} and $E_i^{tot} + \beta$. If a cargo is delivered beyond the grace period, then penalty for shipping delay μ_i is imposed in proportion to the number of delay days $y_{i,\omega}^{del}$ up to δ days. The random weather

Sets and Indices:

S	Set of LNG terminals;
$G(V, A)$	Directed graph nodes $V = \{1,2, ..., i = s + \|S\|r_s - 1)$ where r_s is a delivery sequence number per plant}as the set of plants and $A = \{(i, j): i, j \in V, i \neq j\}$ as the set of arcs in the planning time horizon;
V_1	Set of liquefaction plants where $V_1 = \{1,1 + \|S\|, 1 + 2\|S\|, ..., i_0 = 1 + \|S\|(r_s - 1)$ in the planning horizon $V_1 \subseteq V$;
V_2	Set of regasification plants in the planning time horizon where $V_2 \subseteq V$ and $V_1 \cap V_2 = \emptyset$;
A_1	Set of initial delivery routes where $A_1 = \{(i, j): i \in V_1, j \in V_2\}$ as the set of arcs from a liquefaction plant to a regasification plant where $A_1 \subseteq A$;
A_2	Set of initial intermediate routes where $A_2 = \{(i, j): i, j \in V_2, i \neq j\}$ as the set of arcs between regasification plants where $A_2 \subseteq A$;
A_3	Set of return routes where $A_3 = \{(i, j): i \in V_2, j \in V_1\}$ as the set of arcs from a regasification plant to a liquefaction plant where $A_1 \subseteq A$ and $A_1 \cap A_2 \cap A_3 = \emptyset$;
K_1	Set of type I LNG carriers, $K_1 \subseteq K$;
K_2	Set of type II LNG carriers, $K_2 \subseteq K$, and $K_1 \cap K_2 = \emptyset$;
T	Set of dates;
K	Set of LNG carriers;
Θ	An indicator of the beginning (1) or ending (2) of a weather disruption, Θ= {1,2};
Ω	Set of weather disruption scenarios;

Data:

$E_{i,j}^{tr}$	Estimated travel time from i to j (days);
E_i^{tot}	Expected cargo arrival date at i (days);
δ	Time window - maximum number of delay days from an expected cargo arrival date (days);
L_k^{cp}	Cargo capacity of vessel k (billion cubic meters, or *bcm*);

$L_{i,t,\omega}^{ld}$ Amount of LNG cargo loaded on an LNG carrier heading to initial destination i on date t in accordance with scenario ω (*bcm*);
D_i Demand at plant i (*bcm*);
R Unit revenue of LNG (*bcm*) ($/unit);
C_k^{vsl} Daily shipping cost of a vessel k ($/day);
C^{str} Daily storage cost per bcm ($/day);
C^{prd} Daily production cost per bcm ($/day);
C^{ap} Daily contingency production cost per bcm ($/day);
μ_i Penalty for shipping delay to i ($/day);
γ Maximum number of plants can be visited in a path;
M large-positive number;

Random Elements:

α Barred fill range of LNG carrier type I $[\underline{\alpha}, \overline{\alpha}]$ (%);
β Number of grace (days);
ε Daily boil-off rate (%);
ρ Minimum/maximum storage level $[\underline{\rho}, \overline{\rho}]$ (*bcm*);
ψ Minimum/maximum production level $[\underline{\psi}, \overline{\psi}]$ (*bcm*);
c_t Time index as a constant where $c_t = \{1,2,3,...,t\}$;
$\omega \in \Omega$ A sample point and sample space of weather disruption variations;
$\xi_{i,\omega,\theta}$ A weather disruption beginning time ($\theta = 1$) or ending time ($\theta = 2$) which impacts to an LNG loading time heading to a regasification plant i in accordance with scenario ω;
$\tau_{i,\omega,\theta}$ Departure date from a liquefaction plant to a regasification plant i in accordance with scenario ω where $\tau_{i,\omega,\theta} = E_i^{tot} - E_{i_0,i}^{tr} - \xi_{i,\omega,\theta}$;

Decision Variables:

$x_{i,j}^{lng}$ Amount of LNG cargo from i to j (*bcm*);
$x_{i,j,k}^{vsl}$ $\begin{cases}1, & \text{If vessel } k \text{ maneuvers from } i \text{ to } j;\\ 0, & \text{Otherwise;}\end{cases}$
$x_{i,j,k,\theta}$ $\begin{cases}1, & \text{If vessel } k \text{ traverses from } i \text{ to } j \text{ on date } \theta;\\ 0, & \text{Otherwise;}\end{cases}$
x_t^{prd} Production level on date t (*bcm*);
x_t^{str} Storage level on date t (*bcm*);
$y_{i,\omega}^{tot}$ Vessel arrival date at a regasification plant i in accordance with scenario ω;
$y_{i,\omega}^{del}$ Number of delay days at a regasification plant i in accordance with scenario ω (days);
$y_{t,\omega}^{+}$ Amount of excessive LNG on date t in accordance with scenario ω (*bcm*);
$y_{t,\omega}^{-}$ Amount of LNG shortage on date t in accordance with scenario ω (*bcm*);
u_i The rank-order of plant i in a tour;
$y_{i,t,\omega}^{st}$ $\begin{cases}1, & \text{If an initial destination } i \text{ is visited on date } t \text{ according to scenario } \omega;\\ 0, & \text{Otherwise.}\end{cases}$

disruption timing $\xi_{i,\omega,\theta}$ influencing a voyage of an LNG carrier from a liquefaction plant to a regasification plant $i \in V_2$ is represented by the sampled weather disruption scenarios $\omega \in \Omega$ and probability mass function p_ω. Scheduling a vessel departure time from a liquefaction plant is subject to an expected vessel arrival time at an initial destination E_i^{tot} in a path, travel time between two plants $E_{i,j}^{tr}$ and extreme weather timing $\xi_{i,\omega,\theta}$. Therefore, a vessel departure time from a depot $\tau_{j,\omega,\theta} = E_i^{tot} - E_{i_0,i}^{tr} - \xi_{i,\omega,\theta}\ \forall\ i \in V, i_0 \in V, j \in V, \omega \in \Omega, \theta \in \Theta$. BOG is generated at the constant rate ε and added to the calculation for the amount of loading LNG in a vessel during a laden voyage.

Formulation:

$$\begin{aligned}\text{maximize } & R\Big(\textstyle\sum_{j\in V_2}\sum_{t\in T} D_{j,t} - \sum_{(i,j)\in A}\varepsilon E_{i,j}^{tr} x_{i,j}^{lng}\Big)\\ & - \textstyle\sum_{(i,j)\in A}\sum_{k\in K} C_k^{vsl} E_{i,j}^{tr} x_{i,j,k}^{vsl}\\ & - \textstyle\sum_{t\in T}\left(C^{prd} x_t^{prd} + C^{str} x_t^{str}\right) - |\Omega|^{-1}\sum_{t\in T}\sum_{\omega\in\Omega}\left(C^{ap} y_{t,\omega}^{-} + C^{str} y_{t,\omega}^{+}\right)\\ & - |\Omega|^{-1}\textstyle\sum_{j\in V_2}\sum_{\omega\in\Omega}\mu_j y_{j,\omega}^{del},\end{aligned} \tag{1}$$

subject to:

$$\textstyle\sum_{j\in V}\sum_{k\in K} x_{i,j,k}^{vsl} \le 1,\ \ i \in V_2, \tag{2}$$

$$\textstyle\sum_{i\in V}\sum_{k\in K} x_{i,j,k}^{vsl} \le 1,\ \ j \in V_2, \tag{3}$$

$$x_{i,j,k}^{vsl} \le \textstyle\sum_{l\in V} x_{j,l,k}^{vsl} \le |S| - (|S|-1)x_{i,j,k}^{vsl},\ \ i \in V, j \in V_2, k \in K, \tag{4}$$

$$\sum_{(i,j)\in A_1}\sum_{k\in K} x_{i,j,k}^{vsl} = \sum_{(i,j)\in A_3}\sum_{k\in K} x_{j,i,k}^{vsl}, \tag{5}$$

$$\textstyle\sum_{(i,j)\in A_1} x_{i,j,k}^{vsl} \le 1,\ \ k \in K, \tag{6}$$

$$u_i - u_j + (\gamma+1)\textstyle\sum_{k\in K} x_{i,j,k}^{vsl} \le \gamma,\ \ (i,j) \in A_2, \tag{7}$$

$$x_{i,j}^{lng} \le \textstyle\sum_{k\in K} L_k^{cp} x_{i,j,k}^{vsl},\ \ (i,j) \in A, \tag{8}$$

$$\textstyle\sum_{i\in V}(1-\varepsilon E_{i,j}^{tr}) x_{i,j}^{lng} - D_j = \sum_{l\in V} x_{j,l}^{lng},\ \ j \in V_2, \tag{9}$$

$$x_{i,j}^{lng} \ge \overline{\alpha} L_k^{cp} x_{i,j,k}^{vsl},\ \ (i,j) \in A, k \in K_1, \tag{10}$$

$$x_{i,j}^{lng} \le \underline{\alpha} L_k^{cp} x_{i,j,k}^{vsl},\ \ (i,j) \in A_3, k \in K_1, \tag{11}$$

$$\textstyle\sum_{k\in K} x_{i,j,k}^{vsl} = \sum_{k\in K}\sum_{\theta\in\Theta} x_{i,j,k,\theta},\ \ (i,j) \in A_1, \tag{12}$$

$$\begin{aligned}-M(1-\textstyle\sum_{k\in K} x_{i,j,k}^{vsl}) \le (\tau_{j,\omega,\theta} + E_{i,j}^{tr})\textstyle\sum_{k\in K} x_{i,j,k,\theta} - y_{j,\omega}^{tot}\ \ (i,j) \in A_1, \omega \in \Omega, \theta\in\Theta,\\ \le M(1-\textstyle\sum_{k\in K} x_{i,j,k}^{vsl}),\end{aligned} \tag{13}$$

$$-M(1-\sum_{k\in K} x^{vsl}_{i,j,k}) \le E^{tr}_{i,j}\sum_{k\in K} x^{vsl}_{i,j,k} - y^{tot}_{j,\omega} + y^{tot}_{i,\omega} \quad (i,j)\in A_2,\ \omega\in\Omega, \le M(1-\sum_{k\in K} x^{vsl}_{i,j,k}), \tag{14}$$

$$E^{tot}_i - \delta \le E^{tot}_i + \beta + y^{del}_{i,\omega}, \quad i\in V_2,\ \omega\in\Omega, \tag{15}$$

$$\beta + y^{del}_{i,\omega} \le \delta, \quad i\in V_2,\ \omega\in\Omega, \tag{16}$$

$$x^{str}_t - x^{str}_{t-1} = x^{prd}_t + y^{+}_{t,\omega} - y^{-}_{t,\omega} - \sum_{i\in V_2} L^{ld}_{i,t,\omega}, \quad t\in T,\ \omega\in\Omega, \tag{17}$$

$$(E^{tot}_j - E^{tr}_{i_0,j} - \xi_{j,\omega,\theta})\sum_{k\in K}\sum_{\theta\in\Theta} x^{vsl}_{i_0,j,k,\theta} = c_t \sum_{t\in T} y^{st}_{j,t,\omega}, \quad j\in V_2,\ \omega\in\Omega, \tag{18}$$

$$\sum_{t\in T} y^{st}_{i,t,\omega} \le 1, \quad i\in V_2,\ \omega\in\Omega, \tag{19}$$

$$x^{lng}_{i_0,j} = \sum_{t\in T} L^{ld}_{j,t,\omega}, \quad j\in V_2,\ \omega\in\Omega, \tag{20}$$

$$\underline{\psi} \le x^{prd}_t \le \overline{\psi}, \quad t\in T, \tag{21}$$

$$\underline{\rho} \le x^{str}_t \le \overline{\rho}, \quad t\in T. \tag{22}$$

The objective function (1) consists of five terms. The first term is the lump sum profits for exporting LNG minus the boil-off loss. The second term is the vessel operating costs in proportion to the shipping distance. The third term is the production and inventory cost. The fourth term is the expected cost for additional LNG productions or extended inventories after the realization of a specific weather disruption scenario. The last term is the expected penalty for shipping delays beyond the grace period. The five terms in the objective function are all measurable regarding cost.

Constraint sets (2) through (5) are conditions for LNG carriers' flow balances. Constraint sets (2) and (3) indicates the condition that only one LNG carrier is allocated to meet the demand at any regasification terminal. Constraint set (4) expresses that a route is constructed only when the carrier entering and leaving the terminal is the same. Constraint sets (5) and (6) indicate that the number of LNG carriers departing from a depot is equal to the number of vessels returning to a depot, and each vessel is assigned only once within a given planning time period. Constraint set (7) is the Miller-Tucker- Zemlin (MTZ) sub-tour elimination constraints to construct a complete path for each vessel. More details about the sub-tour elimination methods can be found in (Miller et al., 1960). The constraint set (8) indicates that an LNG load should be less than or equal to the maximum loading capacity of an assigned LNG carrier. Particularly, some of the loaded LNG is lost in BOG form in proportion to shipping time. Therefore, the amount of LNG charged should be calculated considering this loss, and a suitable LNG carrier should be selected as shown in constraint set (9). Since the type I LNG carrier can load or unload within the barred fill range to avoid sloshing effects, constraint sets (10) and (11) specify these conditions.

Constraint sets (12) through (16) are related to the departure time of an LNG carrier from a depot. When an LNG carrier starts a tour from a depot, extreme weather can affect the starting point of the carrier. In this case, the vessel must determine whether to depart before or after the bad weather. The left-hand side (LHS) of constraint (12) is 1 when the route connecting the depot to any regasification plan is selected, and the right-hand side (RHS) is also 1. The RHS of the constraint set (12) has a decision variable $x_{i,j,k,\theta}$ for determining whether the LNG carrier departs before or after the weather disruption, and is associated with constraint sets (13) and (14) to determine the starting point. Constraint sets (13) and (14) calculate the departure time of the LNG carrier from a depot and the arrival time at the first destination considering random weather scenarios. Constraint sets (15) and (16) check whether the LNG carrier arrives at the destination within the grace period. If the vessel arrives after the grace period, the delay is multiplied by the penalty per unit time in the objective function (1) and is calculated as part of the expected cost in the recourse function.

Constraint sets (17) through (22) are related to LNG production and inventory planning to prepare for the ordered amount of LNG on or before the loading date. Constraint set (17) is two-stage production-inventory control constraints that consider a random extreme weather variation in lead time estimation. When the random extreme weather is about to disturb LNG loading operations for a certain length of time, all planned loading tasks must be rescheduled either before or after the extreme event. Changes in LNG loading time will also have an impact on LNG carrier departure time, production and storage plans simultaneously. Therefore, all the time-related data and variables must be synchronized with each other. LNG carrier departure time is expressed in the LHS of constraint set (18). If a route from a depot i_0 to a regasification terminal j is selected, then travel time between the two terminals $E^{tr}_{i_0,j}$ are subtracted from the expected arrival time of an LNG carrier at terminal j E^{tot}_j. The LHS indicates the LNG carrier departure time, and the RHS represents the LNG production and storage completion time to be prepared in accordance with the LNG carrier departure schedule. To synchronize the production-inventory time index t with LNG carrier departure time, time constant c_t is introduced which indicates the index t. For example, if an LNG carrier is heading to a regasification terminal 2 as an initial destination from a depot, expected cargo arrival time at terminal 2 is expressed as $E^{tot}_2 = 20$, and shipping days between two terminals is noted as $E^{tr}_{i_0,2} = 10$. As a result, the LHS value is 10, which means the LNG carrier should start on day 10. Since the value of LHS and RHS must be the same, $\sum_{t\in T} c_t y^{st}_{2,t}$ is 10 where $c_{10} = 10$ and $y^{st}_{2,10} = 1$. Thus, the RHS also indicates the LNG to be loaded into the LNG carrier destined for terminal 2 and should also be ready by day 10. Constraint set (19) indicates a point on the time horizon when a certain demand site i is the first destination of an LNG carrier. Constraint set (20) indicates the amount of LNG cargo to be loaded into an LNG carrier destined for the first destination j that must be prepared by time t, irrespective of the time of any weather scenarios, in conjunction with constraint set (17). Constraint set (21) specifies the maximum production capacity per unit time and the minimum production capacity. Constraint set (22) represents the maximum storage capacity and safety stock level of the LNG storage.

3.1. Computational considerations

In this section, we discuss two computational techniques to improve computational performance supposing that an LNG carrier serves less than two regasification plants $\{i, j\} \in V_2$ in a path. The first approach is a probing-based preprocessing technique (PPT) that reduces the number of binary variables in the model. This technique eliminates both infeasible and inferior routing options in terms of the time window and potential BOG losses in a path. The second one is a logical inequality which eliminates the need for tour sequencing process assuming $\gamma = 2$. We can consider five routing cases listed in Fig. 4.

In Case #1, the time gap between two plants is greater than the estimated travel time $E^{tr}_{i,j}$. Therefore, this routing option is excluded from the model because it makes unnecessary vessel idle time offshore to meet the scheduled port entry time. The time window gap in Case #2 is less than or equal to the estimated travel time from plant i to plant j. Thus an LNG carrier can travel from plant i to j, but not in the reverse direction. Case #3 shows two time windows overlapped and the length of the nested time period is less than or equal to the travel time between two plants. Thus, a vessel can also travel from plant i to j but not in reverse.

In Case #4 and Case #5, the overlapped time duration is greater than or equal to the travel days between two plants. Therefore, an assigned vessel can travel to both. However, recalling equation (21), it is possible to eliminate one of the two routing options by comparing the amount of BOG.

We have a simple illustrative example in Fig. 5. If a vessel travels following sequence (A), $i_0 \to i \to j \to i_0$, then $BOG_{(A)} = 0.00125(\%) \times$

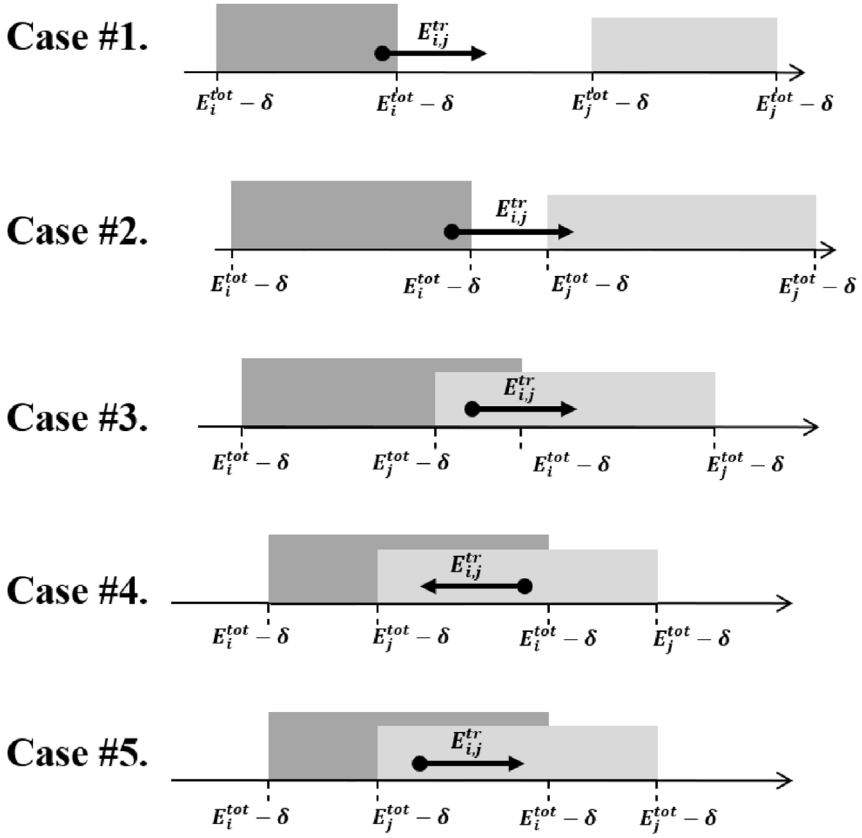

Fig. 4. Five routing cases.

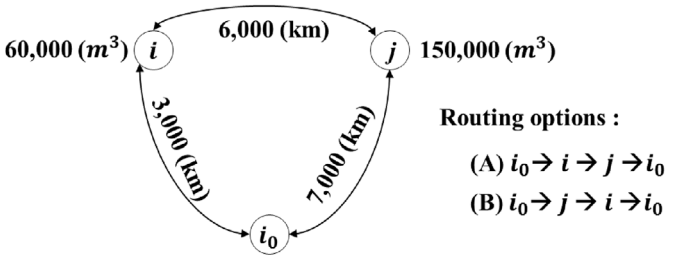

Fig. 5. An illustrative example of routing options serving two regasification plants.

$\{3000 \times (60{,}000 + 150{,}000) + 6{,}000 \times 150{,}000\} = 19{,}125(m^3)$, where daily BOR ε is 0.00125 (%). If it follows sequence (B), $BOG_{(B)} = 0.00125(\%) \times \{7000 \times (60{,}000 + 150{,}000) + 6{,}000 \times 60{,}000\} = 22{,}875(m^3)$. As a result, it is shown that routing option (B) is inferior to (A) and should be excluded from a routing option in the optimization model. Algorithm 1 below provides an overview of the PPT procedure.

The key advantage of our proposed technique is that there is no need for a sequencing process stated by constraint set (8) because only one routing option is available after the PPT procedure is applied. Thus, a logical inequality (23) can replace constraint set (8) in the TSS model. We name the resulting model reinforced PPT (rPPT). The logical operation is shown in Remark 3.1.

$$2\sum_{k\in K} x^{vsl}_{i,j,k} \le \sum_{k\in K} x^{vsl}_{j,i_0,k} + \sum_{k\in K} x^{vsl}_{i_0,i,k}, \quad (i,j) \in A_2. \tag{23}$$

Remark 3.1. Suppose that an assigned LNG carrier departs from a liquefaction plant i_0 and visits two regasification plants i and j in sequence via path a_n: $i_0 \rightarrow i \rightarrow j \rightarrow i_0$ which is the only routing option. Then, $\sum_{k\in K} x^{vsl}_{i,j,k}$ must be equal to 1. If a vessel does not serve i and j together in a path, then $\sum_{k\in K} x^{vsl}_{i,j,k} = 0$.

Algorithm 1 Probing procedure

for all $(i,j) \in A_2$, $k \in K$ **do**
  if $(E^{tot}_j - E^{tot}_i - 2\delta \ge 0)$ **then**
    if $(E^{tot}_j - E^{tot}_i - 2\delta \ge E^{tr}_{i,j})$ **then**
      $\sum_{k\in K} x^{vsl}_{i,j,k} = 0$
      $\sum_{k\in K} x^{vsl}_{j,i,k} = 0$
    else
      $\sum_{k\in K} x^{vsl}_{j,i,k} = 0$
    end if
  else if $(E^{tot}_j - E^{tot}_i - 2\delta \le E^{tr}_{i,j})$ **then**
    $\sum_{k\in K} x^{vsl}_{j,i,k} = 0$
  else if $(BOG_{i,j} \le BOG_{j,i})$ **then**
    $\sum_{k\in K} x^{vsl}_{j,i,k} = 0$
  else
    $\sum_{k\in K} x^{vsl}_{i,j,k} = 0$
  end if
end for

3.2. Decision makers preference model (DMP)

In this section, we present a DMP model that allows a decision maker to make a subjective judgment in response to weather uncertainty affecting LNG IRPs. Unlike the TSS model, the DMP model is formulated as a deterministic optimization model because it takes into account one weather scenario which is generated using a triangular distribution.

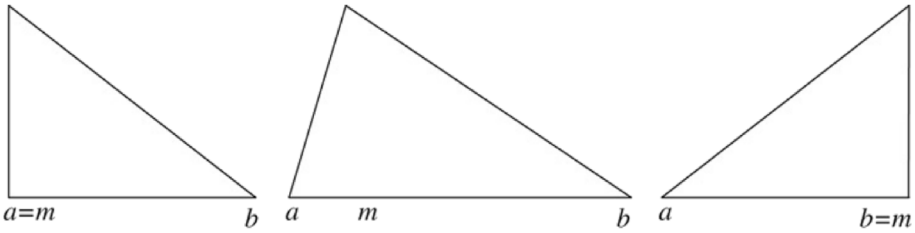

Fig. 6. Three examples of triangular distributions of uncertain weather disruptions. The left graph is the case that corresponds to the minimum of variates. The center graph is the typical triangular density, with mode m. The right graph is the maximum of variates.

The triangular distribution is typically used for subjective analysis of populations when only limited sample data is available. For example, if there is insufficient or unreliable statistical data on weather disruptions to input into the TSS model, it is difficult to produce good-quality weather scenarios. Therefore, the solutions obtained through the TSS model are not likely to have a meaningful value of a stochastic solution. Instead, the DMP model allows intuitive planning using only the least amount of available statistical information, such as the upper and lower limits of weather disruption days, and the most likely weather scenario given by a decision maker.

Assuming that the expected duration of the extreme weather is at least a, maximum b and the most likely duration is mode m, the following types of triangular distributions can be expressed in Fig. 6. When generating weather disruption scenarios to input into the DMP model, the mode value can be adjusted according to the subjective perspective of a decision maker.

Supposing that an LNG supplier wants to put more emphasis on 'on-time delivery', then the priority should be to minimize the expected number of delay days caused by potential weather disruptions. To reflect this risk-averse preference, m must be close to b to generate many scenarios with long durations of extreme weather. As a result, all LNG carriers are planned to depart early considering the relatively long weather disruption period, and the LNG production-storage plan is also prepared accordingly to avoid shipping delays. On the other hand, if a decision maker is risk-prone, m will have a value close to a, so short-term extreme weather scenarios will be generated. If the value of m is changed according to the decision maker's judgment, it ultimately affects the objective value and the schedule. In the DMP model, mode m is selected as a convex combination of the two extreme scenarios reflecting a decision maker's preference by a weight parameter λ $(0 \le \lambda \le 1)$:

$$m = \lambda a + (1 - \lambda) b. \tag{24}$$

In the TSS model, weather disruption time indicator $\xi_{i,\omega,\theta}$ is used to identify a weather disruption beginning time $(\theta = 1)$ or ending time $(\theta = 2)$ which impacts an LNG carrier heading to a regasification plant j in accordance with scenario ω. Since the DMP model considers only one scenario, we use the following weather disruption time indicator $\xi_{i,\theta}$ without random element index ω. The relationship between $\xi_{i,\theta}$ and m is expressed as $\xi_{j,1} + m = \xi_{j,2} \ \ \forall j \in V_2$, and the departure date from a liquefaction plant to a regasification plant is obtained by: $\tau_{j,1} = E_j^{tot} - E_{i_0,j}^{tr} - \xi_{j,1}$, $\tau_{j,2} = E_j^{tot} - E_{i_0,j}^{tr} - \xi_{j,2} \ \forall i_0 \in V, j \in V$.

Let all sets, indices, parameters, and variables be as described before, except that we do not consider the random elements $\omega \in \Omega$ since the problem is formulated as a deterministic optimization model. The DMP model is formulated as follows:

$$\text{maximize } R\left(\sum_{j\in V_2}\sum_{t\in T} D_{j,t} - \sum_{(i,j)\in A} \varepsilon E_{i,j}^{tr} x_{i,j}^{lng}\right) - \sum_{(i,j)\in A}\sum_{k\in K} C_k^{vsl} E_{i,j}^{tr} x_{i,j,k}^{vsl} - \sum_{t\in T}\left(C^{prd} x_t^{prd} + C^{str} x_t^{str}\right) \tag{25}$$

subject to:

Constraint sets (2)–(12), (21), (22),

$$-M\left(1 - \sum_{k\in K} x_{i,j,k}^{vsl}\right) \le \left(\tau_{j,\theta} + E_{i,j}^{tr}\right) \sum_{k\in K} x_{i,j,k,\theta} - y_j^{tot} \le M\left(1 - \sum_{k\in K} x_{i,j,k}^{vsl}\right), \quad (i,j) \in A_1,\ \theta \in \Theta, \tag{26}$$

$$-M\left(1 - \sum_{k\in K} x_{i,j,k}^{vsl}\right) \le E_{i,j}^{tr} \sum_{k\in K} x_{i,j,k}^{vsl} - y_j^{tot} + y_i^{tot} \le M\left(1 - \sum_{k\in K} x_{i,j,k}^{vsl}\right), \quad (i,j) \in A_2, \tag{27}$$

$$E_i^{tot} - \delta \le E_i^{tot} + \beta + y_i^{del}, \ \ i \in V_2, \tag{28}$$

$$\beta + y_i^{del} \le \delta, \ \ i \in V_2, \tag{29}$$

$$x_t^{str} - x_{t-1}^{str} = x_t^{prd} + y_t^{+} - y_t^{-} - \sum_{i\in V_2} L_{i,t}^{ld}, \ \ t \in T, \tag{30}$$

$$\left(E_j^{tot} - E_{i_0,j}^{tr} - \xi_{j,\theta}\right) \sum_{k\in K}\sum_{\theta\in\Theta} x_{i,j,k,\theta}^{vsl} = c_t \sum_{t\in T} y_{j,t}^{st}, \ \ j \in V_2, \tag{31}$$

$$\sum_{t\in T} y_{i,t}^{st} \le 1, \ \ i \in V_2, \tag{32}$$

$$x_{i_0,j}^{lng} = \sum_{t\in T} L_{j,t}^{ld}, \ \ j \in V_2, \tag{33}$$

The mathematical formulation for the DMP model is similar to the TSS model. When comparing the objective functions of both models (1) and (25), The first three terms are the same, but the DMP model does not include the fourth and fifth terms of the TSS model. This is because the TSS model is a two-stage stochastic optimization model and should include recourse functions. However, a recourse function is not required for the DMP model because it is deterministic. Constraint sets (2)–(12), (21), (22) are exactly the same as the constraints from the TSS model. Constraint set (26)–(33) is similar to (13)–(20) but does not include a random element index $\omega \in \Omega$.

The DMP model has the advantage of being able to make decisions with a relatively small amount of statistical data compared to the TSS model. However, if information on the parameter belongs to uncertainty is sufficient, the optimal solution obtained from the DMP model may not be better than the results obtained from the TSS model. The relationship between the TSS model and the DMP model is explained in Remark 3.2.

Remark 3.2. We state the TSS model from (1) through (22) as the compact form: $z = max_{x\in X} Ef(x, \xi)$ where x is the first-stage decision variables, $x_{i,j}^{lng}$, $x_{i,j,k}^{vsl}$, $x_{i,j,k,\theta}$, x_t^{prd}, x_t^{str}, u_i; $x \in X$ denotes the constraint sets of TSS model. ξ is the vector of random parameters, weather disruption scenarios; $f(x, \xi^{\omega})$ is the second-stage cost of LNG shipping preparation for a fixed first-stage schedule x and for the specific realization of ξ^{ω}. Let $x^*(\xi)$ and $z^* = max_{x\in X} Ef(x^*(\xi), \xi)$ be an optimal solution and its corresponding objective value of the TSS model, respectively. Let us represent $\overline{x}(\xi^{pref})$ as an optimal solution of the DMP model and $\overline{z} = max_{x\in X} Ef(\overline{x}(\xi^{pref}), \xi^{pref})$ as its optimal value with the vector of random parameters ξ^{pref} which is determined by a decision maker. Both sets of random parameters, ξ and ξ^{pref}, have same elements which are finite and distinct values within the interval $[a, b]$. In a realization of a scenario, if actual weather disruptions follow the distribution of ξ rather than ξ^{pref}, then the objective value of DMP model is expressed as $\overline{z}^* = max_{x\in X} Ef(\overline{x}(\xi^{pref}), \xi)$. In this situation, $x^*(\xi)$ becomes the optimal solution while $\overline{x}(\xi^{pref})$ is just one feasible solution to the TSS model. Therefore, the following inequality $z^* \ge \overline{z}^*$

Table 1
LNG transportation network characteristics.

	Data	Unit
Time horizon	D + 1 to D + 200	days
Total shipping requests	15	times
LNG carriers (type I/II)	5/10	ships
Storage level	[10,220 K]	bcm
Production level	[10,10 K]	bcm
BOR	0.00125	(%) per day
Barred filling range	≤70	(%)
Grace periods	+10	days
Maximum shipping delays	+10	days

holds true (Halvorsen-Weare et al., 2013).

4. Numerical results and analysis

This section presents the computational results of the proposed models. We first describe the test case and experimental details. Then we discuss the results demonstrating computational outcomes and quality of solutions. Particularly, we analyze the DMP solutions to support effective decision making. We finalize the section by evaluating the computational performance. The experiment is based on a realistic operational data, collected from the LNG vessels. The values used for the parameters of the mathematical models are tabulated in Table 1.

In this experiment, we considered the case of the dust storm in the Persian Gulf as a random element to verify the effectiveness of the proposed LNG IRP models. Especially, we analyze ten years worth of data from 1990 to 1999 provided by Doha International Airport in Qatar. We identified dust storm activity was usually intensive between April and September, and the number of dust storm days occurred each month closely followed a Johnson SB distribution (Rao et al., 2001; Johnson, 1949). We could not find enough statistical data on the duration of the storm, but once a dust storm occurred, it lasted for a few hours to a maximum of five days. Since we do not know the probability distribution related to the duration of dust storm occurrence, we generated scenarios according to the uniform distribution in the interval between 1 and 5 days (Bartlett, 2004; Moses, 2017; Giuggio, 2017). Therefore, it is assumed that the duration of the dust storm occurs uniformly in the interval between 1 and 5 days for the experiment of the two proposed models. Especially, unlike the TSS model, the experiment of the DMP model was conducted to reflect the decision maker's subjective judgment on the duration of dust storms according to a triangular distribution.

As shown in Fig. 7, there are cases in which scenarios affect the LNG shipping preparation schedule while others do not. For example, the dust storm starts at $t-3$ and ends at $t-2$, which does not affect the LNG shipping preparation. However, if a storm starts at $t-3$ and ends at $t+1$, the plan must be adjusted.

Our initial attempt to solve the LNG IRP model using CPLEX 12.6 failed to deliver an optimal solution after 24 h of computations. Therefore, the solution pools algorithm feature in CPLEX was used to speed up the solution process, where groups of feasible solution candidates were accumulated within a specified gap of optimal solutions. We set the relative termination tolerance at 3% and the time limit to 24 h. All of the following experiments were conducted on a 3.00 GHz Intel Xeon machine with 364 GB of memory.

4.1. TSS model

The computational outcomes of the TSS model are composed of two solution sets. The first set is the routing decisions presented in Fig. 8 which include vessel assignments to every path and expected plant arrival and departure times.

The second set of the solution is a two-stage production-inventory schedule. The proposed TSS model consists of the first-stage decisions on a production-inventory schedule and the second-stage decisions on additional production or extended storage after the realization of disruptions as shown in Fig. 9. As illustrated in the graph, the first stage inventory schedule and the first stage production schedule are expressed in every single plan, taking into account uncertain weather scenarios that may occur in the second stage. The production rate adjustment plans for each sampled scenario in the second stage are also shown in the graph. The two-stage production-inventory schedule supports stable long-term production decisions, taking into account future uncertain weather changes, and provides information on the schedule for additional LNG production by scenario.

A finite number of scenarios are used to solve the deterministic equivalent TSS model. There is a trade-off between the number of scenarios used and the corresponding computation time. As there are more scenarios used in the model, the accuracy of estimating the recourse function can be improved. However, using more scenarios beyond a certain threshold may lead to a marginal (or no) gain in the objective value at a significant increase in computation time. Therefore, we conducted a sensitivity analysis to investigate this trade-off between

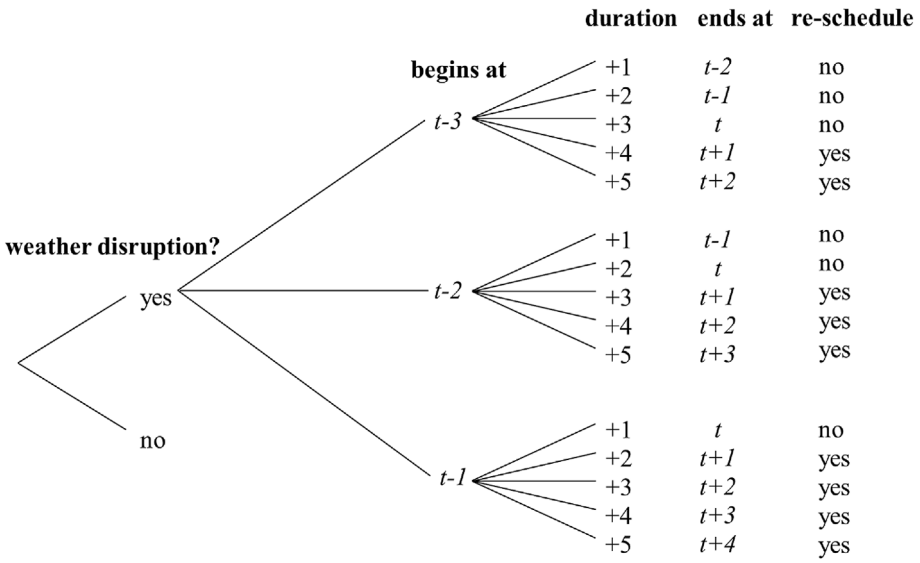

Fig. 7. An example of weather disruption scenario generation.

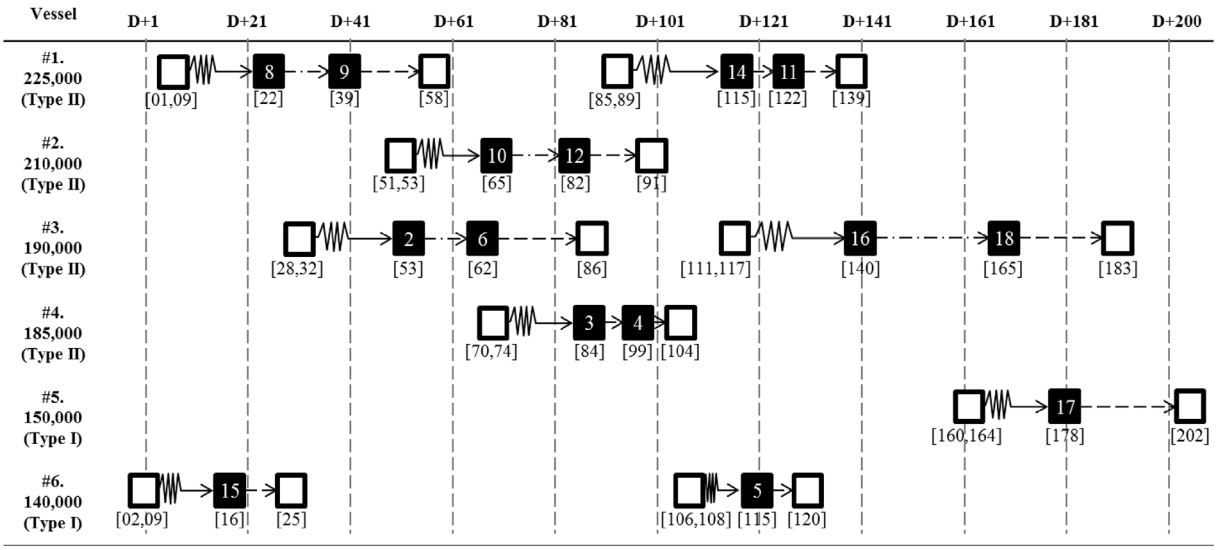

Fig. 8. A shipping schedule.

the number of scenarios and the corresponding objective vlaue. As shown in Fig. 10, the convergence speed steadily decreases as the scenario size increases. For this specific example, about 100 scenarios appear to be a reasonable number to obtain a meaningful solution.

4.2. DMP model

Unlike the TSS model, the DMP model reflects a decision maker's preference as a parameter presented in Fig. 11. In this numerical example, when a decision maker is risk-averse in order to avoid potential delays ($\lambda \rightarrow 1$), then an ordered LNG stock is ready well before potential dust storm disruptions as the production schedule moves to the left in the graph. Conversely, if a decision maker is risk-prone ($\lambda \rightarrow 0$), then the production inventory schedule goes to the right.

Fig. 12 shows the relationship between the preference ratio and the number of delay days in the DMP model. If $\lambda = 0$ (considering the shortest dust storm duration), we can expect the least amount of profit because the planned LNG production inventory schedule and a vessel departure time consider the latest ending time of a dust storm which generates the largest penalty value regardless of random dust storm scenarios. When λ changes from 0.1 to 0.5, there is no significant change in the expected profit but the number of delay days is steadily decreased as λ increases. When λ increases from 0.6 to 1, dust storm scenarios in the early stages influence the problem by generating extended storage costs.

There are three remarkable points in this experiment. First, in the worst case ($\lambda = 0$), profits can significantly drop compared to other preference options. Second, when λ is in between 0.1 and 0.5, if profits are in an acceptable range, then choosing $\lambda = 0.5$ yields reasonable solution because the delay days decreases from 17 to 5 (days). As a result, this what-if analysis can help a decision maker to choose a preferred LNG supply operations plan.

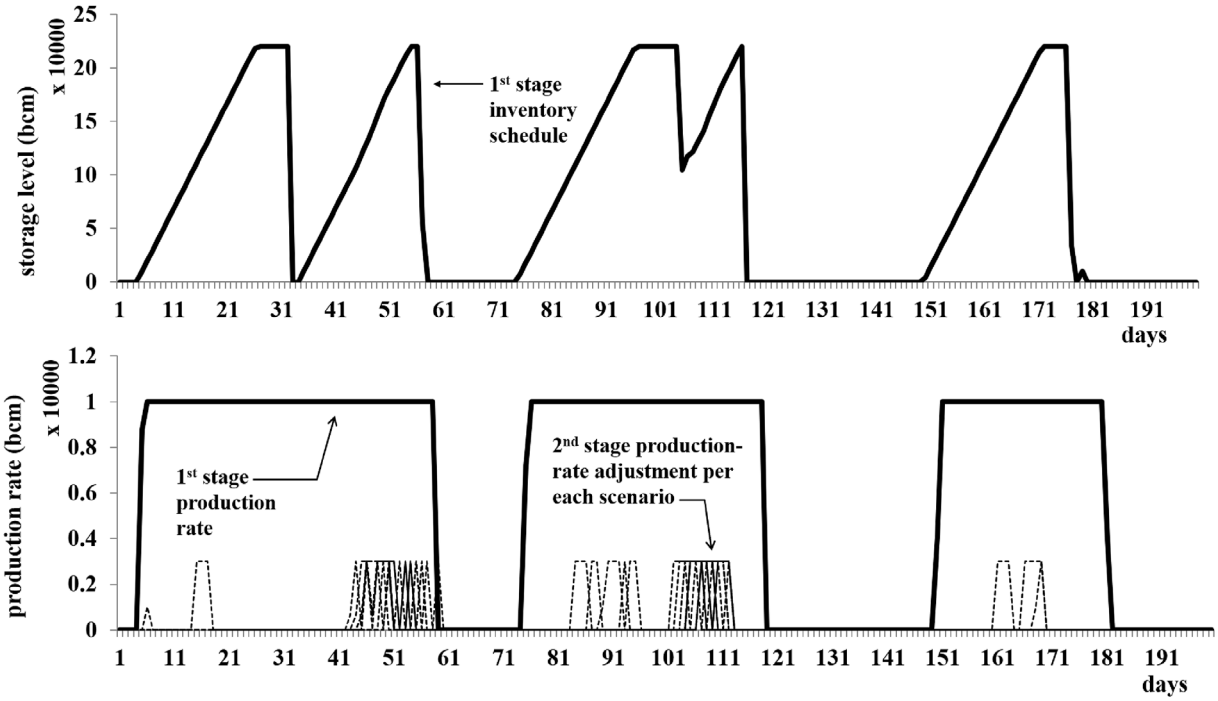

Fig. 9. Two-stage production and inventory schedule.

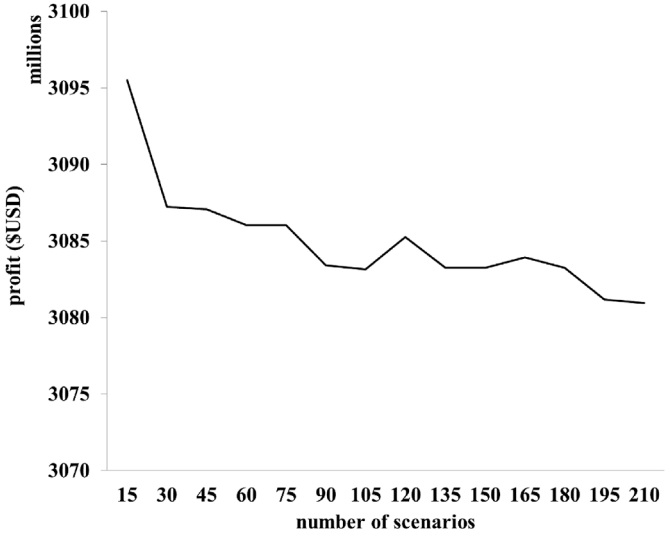

Fig. 10. Expected profit of TSS model per scenario.

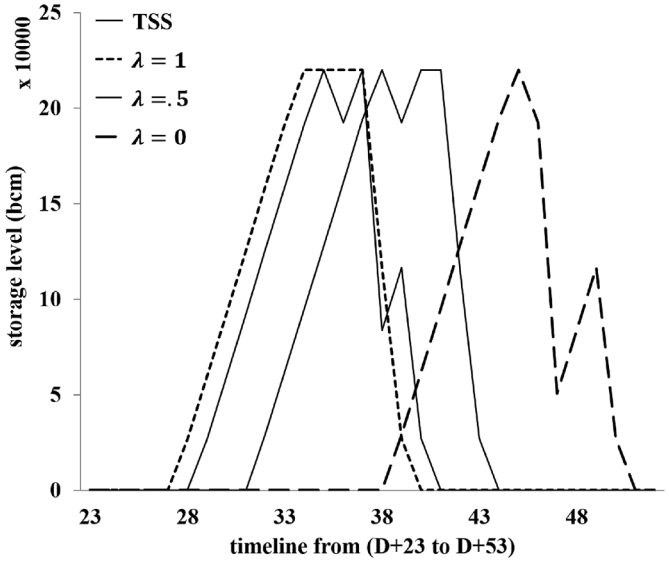

Fig. 11. Production inventory schedule by varying preference ratio on a time horizon.

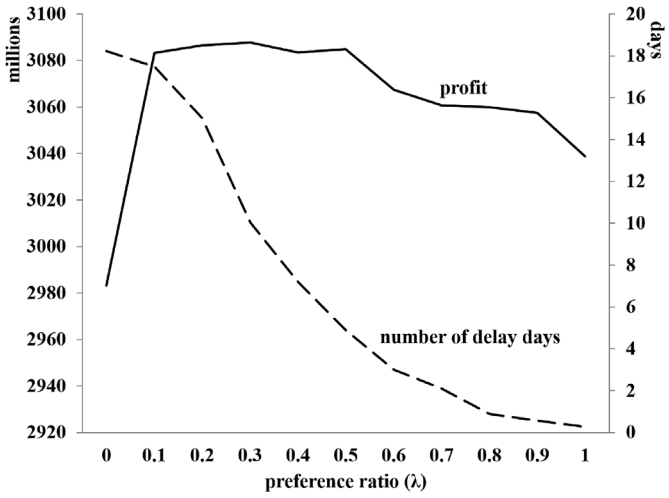

Fig. 12. Profit and number of delay days changing with preference ratio.

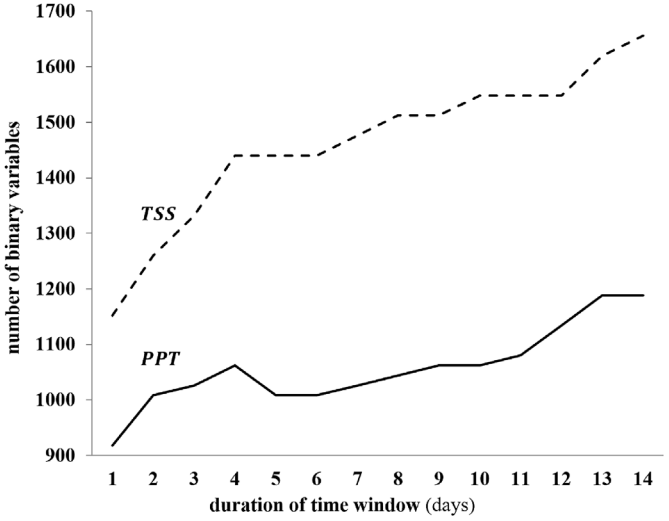

Fig. 13. Number of binary variables of TSS and PPT.

4.3. Computational performance

On our test case, the two optimization models did not return a solution in 24 h. Therefore, we continued our experiments using the probing-based preprocessing technique (PPT) to reduce the number of binary variables. As shown in Fig. 13, the number of binary variables of the TSS model increased as the duration of time window expanded. When PPT is applied, the total number of binary variables has significantly reduced compared to the TSS. For example, when the duration of time window $\beta = 1$, the number of binary variables gap between TSS and PPT was 234 (20.3%); but if $\beta = 10$, the reduction becomes larger at 486 (30.23%).

Further experiments were conducted to test the performance of PPT with the proposed logical inequality (rPPT). Both PPT and rPPT were able to find bluesolution of a good quality within 24 h. As depicted in Fig. 14, there was a positive correlation between the computation time and the scenario size for the problem. Furthermore, there was a maximum 89% reduction in computation time by using rPPT when compared to PPT. This experiment shows a clear advantage of using the proposed logical inequality.

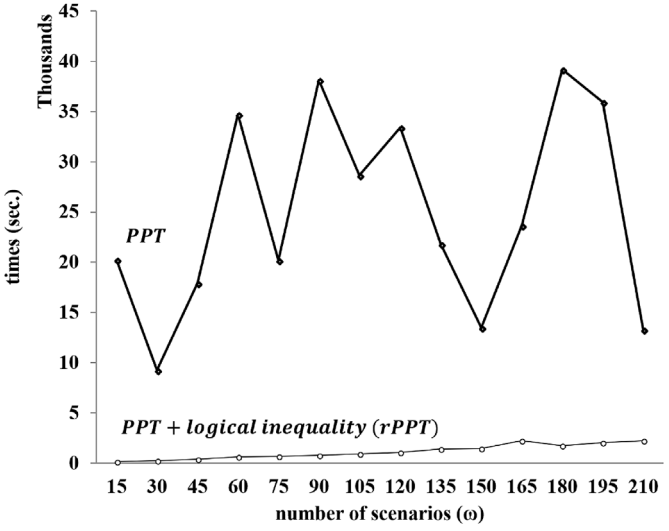

Fig. 14. Computational time vs number of scenarios.

5. Conclusion

In this paper, we proposed two LNG IRP models which are designed to generate optimal routing decisions of LNG carriers and production-inventory schedules that satisfy multiple demands in a path under weather disruptions. The proposed TSS model aimed to maximize the expected profit utilizing weather disruption information derived from historical data. Since the TSS model has a very complex stochastic MIP structure, CPLEX could not solve the problem. However, our probing-based preprocessing technique was successful at reducing the number of binary variables up to 32% utilizing the time windows relations and BOG amount comparisons. Furthermore, the suggested logical inequality performed very stably and efficiently.

The TSS model has five terms in the objective function that are all measurable by monetary value. However, depending on the situation, qualitative factors such as service quality and customer satisfaction may be considered for each objective in addition to the monetary aspects. So, we can develop a multi-objective optimization model with weights that take into account both the quantitative and qualitative importance of each objective.

If historical data on weather disruptions is unreliable or insufficient, the DMP model allows a decision maker's subjective judgment on weather disruption scenario generation. Hence, the DMP model can also be considered as a rational decision supporting methodology compared to the TSS model. In this study, we considered weather disruptions affecting the LNG loading phase at a depot.

By extending this study, we can also study a multi-stage stochastic LNG IRP model that takes into account not only weather disruptions affecting the loading stage in the depot but also the effects of meteorological influences on the unloading stage at the regasification plant.

Acknowledgments

This research was supported in part by the NPRP award [NPRP 4-1249-2-492] from Qatar National Research Fund (a member of the Qatar Foundation).

References

Andersson, H., Christiansen, M., Fagerholt, K., 2010. Transportation planning and inventory management in the LNG supply chain. In: Energy, Natural Resources and Environmental Economics. Springer, pp. 427–439.
Arvesen, O., Medbř, V., Fleten, S.-E., Tomasgard, A., Westgaard, S., 2013. Linepack storage valuation under price uncertainty. Energy 52, 155–164.
Baghalian, A., Rezapour, S., Farahani, R.Z., 2013. Robust supply chain network design with service level against disruptions and demand uncertainties: a real-life case. Eur. J. Oper. Res. 227 (1), 199–215.
Bartlett, K.S., 2004. Dust Storm Forecasting for Al Udeid Ab, qatar: an Empirical Analysis, Ph.D. Thesis. Air Force Institute of Technology.
Bell, W.J., Dalberto, L.M., Fisher, M.L., Greenfield, A.J., Jaikumar, R., Kedia, P., Mack, R.G., Prutzman, P.J., 1983. Improving the distribution of industrial gases with an online computerized routing and scheduling optimizer. Interfaces 13 (6), 4–23.
Canaport, LNG Ship Loading at the Canaport LNG Terminal.
N. Chatterjee, J. Geist, Effects of stratification on boil-off rates in LNG tanks, Pipeline Gas J. 199 (11).
Cho, J., J Lim, G., Biobaku, T., Bora, S., Parsaei, H., 2014a. Liquefied natural gas ship route planning model considering market trend change. Trans. Marit. Sci. 3 (02), 119–130.
Cho, J., Lim, G.J., Biobaku, T., Bora, S., Parsaei, H., 2014b. Liquefied natural gas (LNG) inventory routing problem under weather disruptions: a case study of dust storm in the Persian Gulf. In: THC 2014 Conference. Texas Hurricane Center, Houston, USA.
Christiansen, M., Fagerholt, K., Nygreen, B., Ronen, D., 2013. Ship routing and scheduling in the new millennium. Eur. J. Oper. Res. 228 (3), 467–483.
Coelho, L.C., Laporte, G., 2013. A branch-and-cut algorithm for the multi-product multi-vehicle inventory-routing problem. Int. J. Prod. Res. 51 (23–24), 7156–7169.
Dobrota, D., Lali'c, B., Komar, I., 2013. Problem of boil-off in LNG supply chain. Trans. Marit. Sci. 2 (02), 91–100.
Engineer, F.G., Furman, K.C., Nemhauser, G.L., Savelsbergh, M.W., Song, J.-H., 2012. A branch-price-and-cut algorithm for single-product maritime inventory routing. Oper. Res. 60 (1), 106–122.
Federgruen, A., Zipkin, P., 1984. Computational issues in an infinite-horizon, multi-echelon inventory model. Oper. Res. 32 (4), 818–836.
Finley, M., 2014. BP Statistical Review of World Energy. Tech. rep., BP Technical Report.
Fodstad, M., Uggen, K.T., Rømo, F., Lium, A.-G., Stremersch, G., Hecq, S., 2010. LNG scheduler: a rich model for coordinating vessel routing, inventories and trade in the liquefied natural gas supply chain. J. Energy Market. 3 (4), 31–64.
V. Giuggio, How Dust Storms Work < https://science.howstuffworks.com/nature/climate-weather/storms/dust-storm3.htm > Ω(accessed 11.01.2017).
Goel, V., Furman, K.C., Song, J.-H., El-Bakry, A.S., 2012. Large neighborhood search for LNG inventory routing. J. Heuristics 18 (6), 821–848.
Goel, V., Slusky, M., van Hoeve, W.-J., Furman, K., Shao, Y., 2015. Constraint programming for LNG ship scheduling and inventory management. Eur. J. Oper. Res. 241 (3), 662–673.
Grønhaug, R., Christiansen, M., 2009. Supply chain optimization for the liquefied natural gas business. In: Innovations in Distribution Logistics. Springer, pp. 195–218.
Grønhaug, R., Christiansen, M., Desaulniers, G., Desrosiers, J., 2010. A branch-and-price method for a liquefied natural gas inventory routing problem. Transport. Sci. 44 (3), 400–415.
Halvorsen-Weare, E.E., Fagerholt, K., Rönnqvist, M., 2013. Vessel routing and scheduling under uncertainty in the liquefied natural gas business. Comput. Ind. Eng. 64 (1), 290–301.
Hartley, P.R., 2014. Tech. rep., Working Paper In: Baker IIIJames A. (Ed.), Recent Developments in LNG Markets. Institute for Public Policy, Rice University.
Hartley, P.R., Mitchell, G., Mitchell, C., Baker, J.A., 2013. The Future of Long-term LNG Contracts. University of Western Australia, Business School, Economics.
Higle, J.L., Bean, J.C., Smith, R.L., 1990. Deterministic equivalence in stochastic infinite horizon problems. Math. Oper. Res. 15 (3), 396–407.
Johnson, N.L., 1949. Systems of frequency curves generated by methods of translation. Biometrika 149–176.
Kuo, J., Campbell, R., Ding, Z., Hoie, S., Rinehart, A., Sandström, R., Yung, T., Greer, M., Danaczko, M., et al., 2009. LNG tank sloshing assessment methodology - the new generation. Int. J. Offshore Polar Eng. 19 (4), 241.
Michot Foss, M., 2007. I. 30 (08). Ntroduction to LNG–an Overview on Liquefied Natural Gas (LNG), its Properties, Organization of the LNG Industry and Safety Considerations. Centre for Energy Economics, University of texas, Centre for Energy Economics. University of Texas 2014.
Miller, C.E., Tucker, A.W., Zemlin, R.A., 1960. Integer programming formulation of traveling salesman problems. J. ACM 7 (4), 326–329.
M. Moses, Forecasting Dust Storms in Iraq < http://www.theweatherprediction.com/weatherpapers/111/index.html > Ω(accessed 11.01.2017).
Papageorgiou, D.J., Keha, A.B., Nemhauser, G.L., Sokol, J., 2014. Two-stage decomposition algorithms for single product maritime inventory routing. Inf. J. Comput. 26 (4), 825–847.
D. J. Papageorgiou, M.-S. Cheon, G. Nemhauser, J. Sokol, Approximate dynamic programming for a class of long-horizon maritime inventory routing problems, Transport. Sci..
Qatar Petroleum, Port Information and Regulation Guide.
Rakke, J.G., Stålhane, M., Moe, C.R., Christiansen, M., Andersson, H., Fagerholt, K., Norstad, I., 2011. A rolling horizon heuristic for creating a liquefied natural gas annual delivery program. Transport. Res. C Emerg. Technol. 19 (5), 896–911.
Rao, P.G., Al-Sulaiti, M., Al-Mulla, A.H., 2001. Winter shamals in Qatar, arabian gulf. Weather 56 (12), 444–451.
Rudman, M., Cleary, P.W., 2009. Modelling sloshing in LNG tanks. In: Seventh International Conference on CFD in the Minerals and Process Industries, Australia.
Stålhane, M., Rakke, J.G., Moe, C.R., Andersson, H., Christiansen, M., Fagerholt, K., 2012. A construction and improvement heuristic for a liquefied natural gas inventory routing problem. Comput. Ind. Eng. 62 (1), 245–255.
Thomas, S., Dawe, R.A., 2003. Review of ways to transport natural gas energy from countries which do not need the gas for domestic use. Energy 28 (14), 1461–1477.
Tusiani, M.D., Shearer, G., 2007. LNG: a Nontechnical Guide. PennWell Books.
UNEP Global Environmental Alert Service, Forecasting and Early Warning of Dust Storms.
U.S. Department of Energy, 2005. Liquefied Natural Gas: Understanding the Basic Facts.
U.S. Energy Information Administration, Annual Energy Outlook 2014 with Projections to 2040.
Vidović, M., Popović, D., Ratković, B., 2014. Mixed integer and heuristics model for the inventory routing problem in fuel delivery. Int. J. Prod. Econ. 147, 593–604.
Von Hirschhausen, C., Neumann, A., 2008. Long-term contracts and asset specificity revisited: an empirical analysis of producer–importer relations in the natural gas industry. Rev. Ind. Organ. 32 (2), 131–143.
C. Zhang, G. Nemhauser, J. Sokol, M. Cheon, D. Papageorgiou, Robust Inventory Routing with Flexible Time Window Allocation < http://www.optimization-online.org/DB_FILE/2015/01/4744.pdf/ > (accessed 04.01.2015).